ISSN 1070-3284, Russian Journal of Coordination Chemistry, 2023, Vol. 49, No. 12, pp. 807–811. © Pleiades Publishing, Ltd., 2023.
Russian Text © The Author(s), 2023, published in Koordinatsionnaya Khimiya, 2023, Vol. 49, No. 12, pp. 767–771.

Trimethylammonium Dichlorohexachlorotellurate(IV): Crystal Structure and Specific Features of Noncovalent Cl···Cl Interactions

A. N. Usol'tsev[a, *], **A. A. Sonina**[b], **N. A. Korobeinikov**[a, c], **and S. A. Adonin**[a, d]

[a] *Nikolaev Institute of Inorganic Chemistry, Siberian Branch, Russian Academy of Sciences, Novosibirsk, Russia*
[b] *Vorozhtsov Institute of Organic Chemistry, Siberian Branch, Russian Academy of Sciences, Novosibirsk, Russia*
[c] *Novosibirsk State University, Novosibirsk, Russia*
[d] *Favorskii Institute of Chemistry, Siberian Branch, Russian Academy of Sciences, Irkutsk, Russia*
**e-mail: usoltsev@niic.nsc.ru*

Received January 13, 2023; revised January 31, 2023; accepted February 15, 2023

Abstract—The reaction of tellurium(IV) oxide with trimethylammonium chloride in the presence of gaseous chlorine in concentrated hydrochloric acid gives supramolecular dichlorohexachlorotellurate $(Me_3NH)_2\{[TeCl_6](Cl_2)\}$ (**I**), whose structure is determined by X-ray diffraction (XRD) (CIF file CCDC no. 2217752). The data of elemental and XRD analyses suggest a restricted stability of the synthesized compound. Specific features of noncovalent Cl···Cl interactions in the crystal structure of compound **I** are studied by Raman spectroscopy.

Keywords: tellurium, halide complexes, XRD, halogen bond, noncovalent interactions

DOI: 10.1134/S1070328423600213

INTRODUCTION

Although more than 200 years have passed since the description of the first polyhalide compound [1], this field of research continues to attract attention of scientists [2–7]. The maximum data body was accumulated for polyiodides [8–13], the data on polybromides are appreciably less, and polychlorides and polyfluorides remain weakly studied. A splash of interest in this field accompanied by obtaining a number of interesting experimental results is observed in the recent years. On the one hand, a series of polychlorides with anions of the composition from $\{Cl_3\}^-$ to $\{Cl_{20}\}^{2-}$ was synthesized and characterized [14–18].

On the other hand, a number of important results concerning supramolecular hybrids of anionic halometallates [19–21] and polyhalide fragments was synthesized recently. For instance, polyiodides–iodometallates were shown [22–24] to be a class of compounds characterized by a large variety of structural types. These complexes demonstrate optical properties due to which they are attractive from the viewpoint of a possible use in photovoltaics. As a rule, specific features of binding between halometallate and polyhalide fragments in these compounds are described in the framework of the halogen bond concept [25–28].

The first and to the recent time single example of supramolecular dichloro-chlorometallate was presented about 30 years ago [29] $((Me_4N)_2\text{-}\{[MCl_6](Cl_2)_x\}$, where M = Sn, Pd; $x \leq 1$). We synthesized structurally related complexes of other elements (Te(IV) [30] and Pb(IV) [31]) within recent three years. It was shown that dichloro-chlorometallates of quite different structural types can be formed [32, 33].

Continuing these studies, we synthesized new dichlorohexachlorotellurate(IV): $(Me_3NH)_2\{[TeCl_6]\text{-}(Cl_2)\}$ (**I**). The structural features were studied by XRD, and noncovalent Cl···Cl interactions in compound **I** were revealed by Raman spectroscopy.

EXPERIMENTAL

Concentrated hydrochloric acid (special purity grade) was used. Tellurium(IV) oxide was synthesized by the oxidation of metallic tellurium with concentrated nitric acid (reagent grade). Gaseous chlorine was prepared by the reaction of concentrated HCl and potassium permanganate (high-purity grade) and used without additional drying.

Synthesis of $(Me_3NH)_2\{[TeCl_6](Cl_2)\}$. Weighed samples of tellurium(IV) oxide (81 mg, 0.5 mmol) and trimethylammonium chloride (95 mg, 1 mmol) were dissolved in concentrated HCl (4 mL) on heating (60°C). Then a Cl_2 current was passed through the solution for 15 min. Well cut yellow crystals of com-

Table 1. Crystallographic data and experimental and structure refinement parameters for complex **I**

Parameter	Value
Empirical formula	$Cl_6Te{\cdot}Cl_2{\cdot}2(C_3H_{10}N)$
FW	531.44
Crystal system	Monoclinic
Space group	*Cc*
a, Å	16.2069(9)
b, Å	9.4586(4)
c, Å	13.5204(8)
β, deg	112.539(2)
V, Å^3	1914.3(2)
Z	4
ρ_{calc}, g cm^{-3}	1.844
μ, mm^{-1}	2.66
F(000)	1032.0
Crystal size, mm	0.1 × 0.07 × 0.06
Range of indices *hkl*	$-21 \le h \le 19$, $-11 \le k \le 12$, $-11 \le l \le 17$
Range of data collection over 2θ, deg	5.094–57.378
Number of measured, independent, and observed ($I > 2\sigma(I)$) reflections	6124, 3413, 3251
R_{int}	0.044
Number of refined parameters/number of restraints	160/2
$R(F^2 > 2\sigma(F^2))$, $wR(F^2)$, S	0.049, 0.123, 1.08
Residual electron density (max/min), e/Å^3	1.14/–1.99
Flack X	0.05(5)

pound **I** were formed in 60 min on slow cooling. The yield was 65%.

For $C_6H_{20}N_2Cl_8Te$

Anal. calcd., %	C, 13.56	H, 3.79	N, 5.27
Found, %	C, 13.77	H, 3.89	N, 5.38

XRD of a single crystal of complex **I** was carried out at 150 K on a Bruker D8 Venture diffractometer with a CMOS PHOTON III detector (graphite monochromator, MoK_α radiation, λ = 0.71073 Å, φ and ω scan modes). Integration, absorption correction applying, and unit cell parameter determination were performed using the CrysAlisPro software. The structure was solved using the SHELXT program and refined by full-matrix least squares in the anisotropic (except for hydrogen atoms) approximation using the SHELXL program [34]. The positions of the hydrogen atoms of the organic fragments were calculated geometrically and refined by the riding model. The crystallographic data and experimental details are given in Table 1.

The full set of XRD parameters for compound **I** was deposited with the Cambridge Crystallographic Data Centre (CIF file CCDC no. 2217752; https://www.ccdc.cam.ac.uk/structures/).

Phase XRD of the sample was carried out on a Shimadzu XRD-7000 diffractometer (CuK_α, Ni filter, OneSight linear detector, 2θ = 5°–50°, increment 0.0143° 2θ, acquisition number 2 s per point). The sample was prepared as follows. Polycrystals were triturated in an agate mortar in the presence of heptane, and the obtained suspension was deposited on the polished side of a standard quartz cell. After heptane evaporated, the sample was a thin smooth layer ~100 μm thick. All peaks on the diffraction patterns of compound **I** were indexed by the single-crystal data.

Raman spectroscopy. The spectra were recorded at room temperature in a range of 10–550 cm^{-1} on a LabRAM HR Evolution FT-IR spectrometer (Horiba) equipped with He–Ne and Nd:YAG lasers (λ = 633 and 1064 nm, respectively) and a Ge detector. The sample was prepared as follows: the mother liquor was decanted, and the formed crystalline precipitate was dried between filter paper sheets without rough mechanical action to avoid the decomposition of the crystals. After this, the sample was placed on the

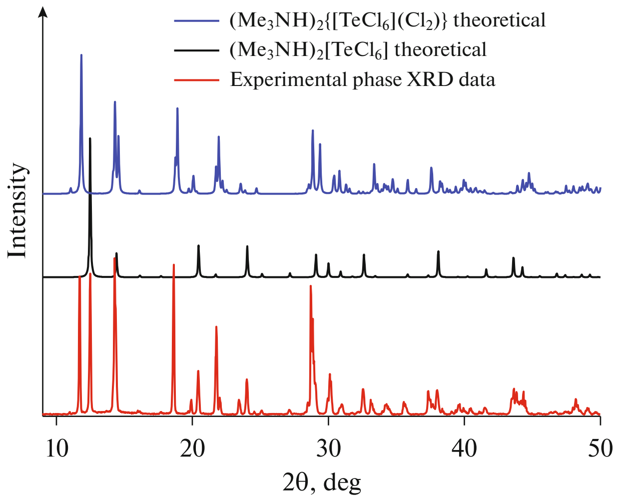

Fig. 1. Comparison of the experimental XRD pattern (red) with the theoretical XRD pattern for compound **I** (blue) and $(Me_3NH)_2[TeCl_6]$ [35] (black).

spectrometer support without grinding, and the Raman spectrum was recorded.

RESULTS AND DISCUSSION

Compound **I** was synthesized via the scheme similar to that used previously for other dichloro-chlorometallates (dissolution of the precursors in concentrated HCl and purging Cl_2 excess in an open system in air). In spite of the fact that the elemental analysis data for the freshly prepared sample of compound **I** coincide with the theoretical values, we failed to obtain a single-phase sample. It is most likely that a strong grinding of the sample during preparation to the XRD experiment significantly accelerates its decomposition. About 50% (estimated visually from the relative value of the peaks) phase of $(Me_3NH)_2[TeCl_6]$, whose structure was described earlier [35], can be observed on the XRD pattern detected (Fig. 1).

According to the XRD data, complex **I** crystallizes in the monoclinic crystal system with the space group of symmetry *Cc*. The crystal packing along the *b* axis is shown in Fig. 2. The independent part of the cell of this compound contains two trimethylammonium cations, one $[TeCl_6]^{2-}$ octahedron, and one Cl_2 molecule (Fig. 3). The main specific feature of compound **I** is the presence of noncovalent interactions $Cl_{term}\cdots Cl_{\{Cl_2\}}$ (2.980(4)–3.02(5) Å) at the distances much shorter than the sum of the van der Waals radii according to Bondi (3.50 Å [36, 37]). The $Cl_{term}\cdots Cl_{Cl_2}-Cl_{Cl_2}$ angles are 172.2(2)° and 170.6(2)°. The $[TeCl_6]^{2-}$ octahedra are distorted: the Te–Cl bonds for the chloride ligands linked with the $\{Cl_2\}$ fragments are longer (2.633(3)–2.652(3) Å vs. 2.443(3)–2.527(4) Å). Owing to the halogen bond, the anionic moiety of this compound can be considered as a one-dimensional zigzag polymer (Fig. 4). In addition, there are hydrogen bonds between the cation and anionic moiety, and their geometric characteristics are given in Table 2. Polychlorotellurate **I** is isostructural to the similar polybromobromotellurate(IV) $(Me_3NH)_2\{[TeBr_6](Br_2)\}$ characterized earlier [38].

In spite of the low stability of compound **I**, we succeeded in detecting its Raman spectrum (Fig. 5). Its main feature is the presence of the high-intensity broad band at 499–504 cm^{-1} corresponding to vibrations of the $\{Cl_2\}$ fragments. As compared to the spectra of solid Cl_2 (containing a triplet of vibrations due to specific features of the isotopic composition of chlorine: 522, 530, and 538 cm^{-1} [39]), this band is noticeably shifted toward lower wavenumbers, which is a common property of the polychlorometallates [30–33] synthesized at the moment and indicates a strong

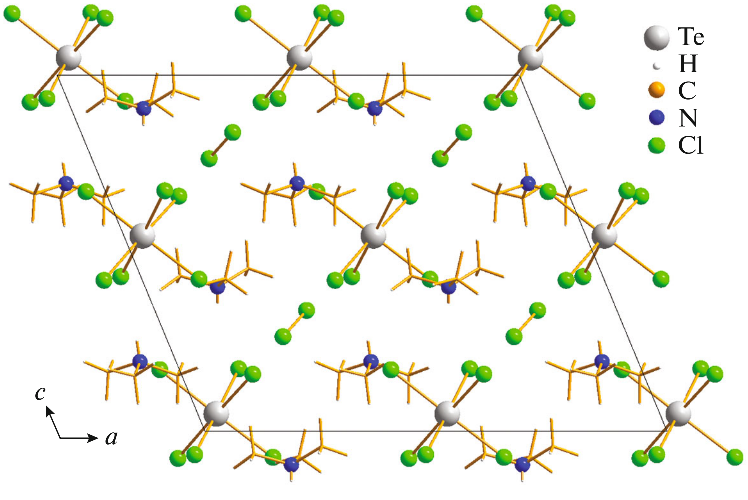

Fig. 2. Crystal packing of compound **I** along the crystallographic *b* axis.

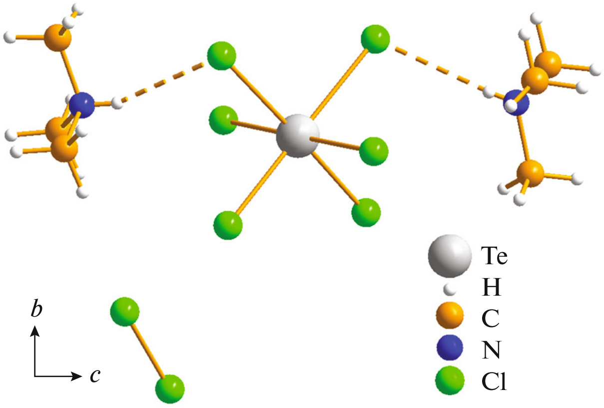

Fig. 3. Fragment of the independent part of the cell along the crystallographic *a* axis and intermolecular interactions of compound **I**.

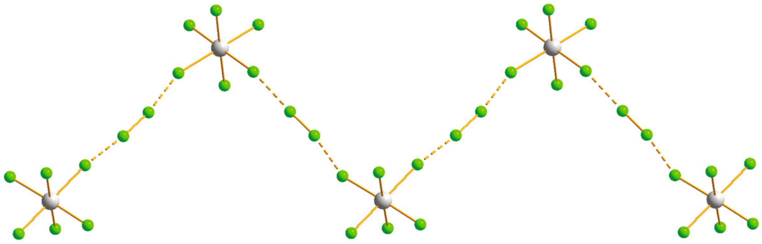

Fig. 4. Zigzag chains in the anionic moiety of compound **I**.

noncovalent interaction between the chlorine molecule and terminal chloride ligands. The bands at 134 and 242 cm^{-1} and the broadened band at 280–292 cm^{-1} correspond to stretching vibrations of the $[TeCl_6]^{2-}$ octahedron and are consistent with the published data for the tellurium compounds with both organic [40] and inorganic cations [41].

To conclude, the new representative of the polychlorometallate family with the trimethylammonium cation was synthesized. Compound **I** demonstrates a restricted stability. The Raman spectrum of compound **I** was detected. The noncovalent Cl···Cl interactions are observed in the crystal structure of compound **I**.

ACKNOWLEDGMENTS

The authors are grateful to the Center for Collective Use of the Nikolaev Institute of Inorganic Chemistry (Siberian Branch, Russian Academy of Sciences) for a possibility of obtaining the initial XRD data.

FUNDING

This work was supported by the Russian Science Foundation (project no. 18-73-10040) and the Ministry of Science and Higher Education of the Russian Federation (structural characterization of the samples, project no. 121031700313-8).

Table 2. Geometric parameters of the hydrogen bond for complex **I**

N–H···Cl	Distance, Å			Angle N–H···A, deg
	N–H	H···Cl	N···Cl	
N(1)–H(1)···Cl(1)	1.00	2.44	3.26(1)	139
N(1)–H(1)···Cl(6)	1.00	2.81	3.57(2)	133
N(2)–H(2)···Cl(2)	1.00	2.31	3.24(1)	154

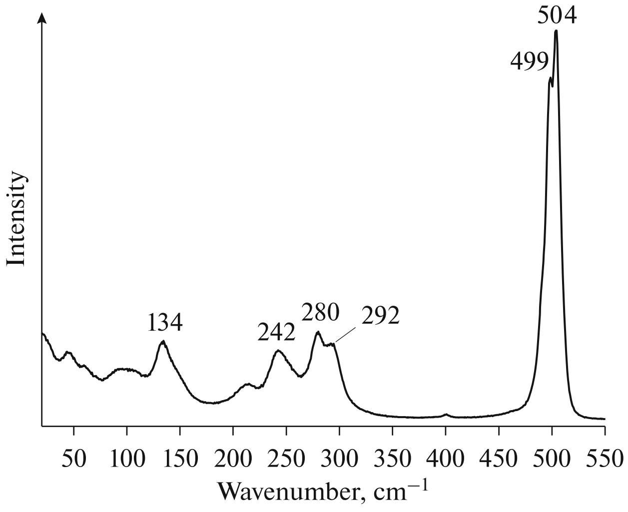

Fig. 5. Raman spectrum of compound **I**.

CONFLICT OF INTEREST

The authors of this work declare that they have no conflicts of interest.

REFERENCES

1. Pelletier, J. and Caventou, J., *Ann Chim Phys*, 1819, vol. 10, p. 142.
2. Yushina, I., Tarasova, N., Kim, D., et al., *Crystals*, 2019, vol. 9, no. 10, p. 506.
3. Bol'shakov, O.I., Yushina, I.D., Stash, A.I., et al., *Struct. Chem.*, 2020, vol. 31, no. 5, p. 1729.
4. Reiss, G.J. and Leske, P.B., *Z. Krist-New Cryst. Struct.*, 2014, vol. 229, no. 4, p. 452.
5. Reiss, G.J., *Z. Krist-New Cryst. Struct.*, 2019, vol. 234, no. 4, p. 737.
6. Reiss, G.J., *Z. Naturforsch., A: Phys. Sci.*, 2015, vol. 70, no. 10, p. 735.
7. Sonnenberg, K., Mann, L., Redeker, F.A., et al., *Angew. Chem., Int. Ed. Engl.*, 2020, vol. 59, no. 14, p. 5464.
8. Haller, H. and Riedel, S., *Z. Anorg. Allg. Chem.*, 2014, vol. 640, no. 7, p. 1281.
9. Savinkina, E.V., Golubev, D.V., and Grigoriev, M.S., *J. Coord. Chem.*, 2019, vol. 72, no. 2, p. 347.
10. Shestimerova, T.A., Bykov, A.V., Kuznetsov, A.N., et al., *Z. Anorg. Allg. Chem.*, 2022, vol. 648, no. 15, p. e202200039.
11. Shestimerova, T.A., Golubev, N.A., Bykov, M.A., et al., Molecules, 2021, vol. 26, no. 18, p. 5712.
12. Kalle, P. and Bezzubov, S.I., *Russ. J. Inorg. Chem.*, 2021, vol. 66, no. 11, p. 1682 https://doi.org/10.1134/S0036023621110103
13. Shestimerova, T.A., Bykov, M.A., Wei, Z., et al., *Russ. Chem. Bull.*, 2019, vol. 68, no. 8, p. 1520.
14. Brückner, R., Haller, H., Ellwanger, M., and Riedel, S., – *Chem. A Eur. J.*, 2012, vol. 18, no. 18, p. 5741.
15. Brückner, R., Haller, H., Steinhauer, S., et al., *Angew. Chem., Int. Ed. Engl.*, 2015, vol. 54, no. 51, p. 15579.
16. Brückner, R., Pröhm, P., Wiesner, A., et al., *Angew. Chem., Int. Ed. Engl.*, 2016, vol. 55, no. 36, p. 10904.
17. Sonnenberg, K., Pröhm, P., Schwarze, N., et al., *Angew. Chem., Int. Ed. Engl.*, 2018, vol. 57, no. 29, p. 9136.
18. Voßnacker, P., Keilhack, T., Schwarze, N., et al., *Eur. J. Inorg. Chem.*, 2021, vol. 2021, no. 11, p. 1034.
19. Fateev, S.A., Khrustalev, V.N., Simonova, A.V., et al., *Russ. J. Inorg. Chem.*, 2022, vol. 67, no. 7, p. 997. https://doi.org/10.1134/S0036023622070087
20. Fateev, S.A., Stepanov, N.M., Petrov, A.A., et al., *Russ. J. Inorg. Chem.*, 2022, vol. 67, no. 7, p. 992. https://doi.org/10.1134/S0036023622070075
21. Petrov, A.A., Marchenko, E.I., Fateev, S.A., et al., *Mendeleev Commun.*, 2022, vol. 32, no. 3, p. 311.
22. Shestimerova, T.A., Yelavik, N.A., Mironov, A.V., et al., *Inorg. Chem.*, 2018, vol. 57, no. 7, p. 4077.
23. Shestimerova, T.A., Mironov, A.V., Bykov, M.A., et al., *Molecules*, 2020, vol. 25, no. 12.
24. Shestimerova, T.A., Golubev, N.A., Yelavik, N.A., et al., *Cryst. Growth Des.*, 2018, vol. 18, no. 4, p. 2572.
25. Desiraju, G.R., Shing, Ho P., Kloo, L., et al., *Pure Appl. Chem.*, 2013, vol. 85, no. 8, p. 1711.
26. Eliseeva, A.A., Ivanov, D.M., Novikov, A.S., et al., *Dalton Trans.*, 2020, vol. 49, no. 2, p. 356.
27. Eliseeva, A.A., Ivanov, D.M., Novikov, A.S., and Kukushkin, V.Yu., *CrystEngComm*, 2019, vol. 21, no. 4, p. 616.
28. Dabranskaya, U., Ivanov, D.M., Novikov, A.S., et al., *Cryst. Growth Des.*, 2019, vol. 19, no. 2, p. 1364.
29. Storck, P. and Weiss, A., *Z. Naturforsch, B: J. Chem. Sci.*, 1991, vol. 46, no. 9, p. 1214.
30. Usoltsev, A.N., Adonin, S.A., Kolesov, B.A., et al., *Chem., A Eur. J.*, 2020, vol. 26, no. 61, p. 13776.
31. Usoltsev, A.N., Korobeynikov, N.A., Kolesov, B.A., et al., *Inorg. Chem.*, 2021, vol. 60, no. 6, p. 4171.
32. Korobeynikov, N.A., Usoltsev, A.N., Kolesov, B.A., et al., *CrystEngComm*, 2022, vol. 24, no. 17, p. 3150.
33. Usoltsev, A.N., Korobeynikov, N.A., Kolesov, B.A., et al., *Chem., A Eur. J.*, 2021, vol. 27, no. 36, p. 9292.
34. Sheldrick, G.M., *Acta Crystallogr., Sect. C: Struct. Chem.*, 2015, vol. 71, no. 1, p. 3.
35. Ben Ghozlen, M.H. and Bats, J.W., *Acta Crystallogr., Sect. B: Struct. Crystallogr. Cryst. Chem.*, 1982, vol. 38, no. 4, p. 1308.
36. Bondi, A., *J. Phys. Chem.*, 1966, vol. 70, no. 9, p. 3006.
37. Mantina, M., Chamberlin, A.C., Valero, R., et al., *J. Phys. Chem.*, 2009, vol. 113, no. 19, p. 5806.
38. Usoltsev, A.N., Adonin, S.A., Abramov, P.A., et al., *Eur. J. Inorg. Chem.*, 2018, vol. 2018, no. 27, p. 3264.
39. Anderson, A. and Sun, T.S., *Chem. Phys. Lett.*, 1970, vol. 6, no. 6, p. 611.
40. Baker, L.-J., Rickard, C.E.F., and Taylor, M.J., *Polyhedron*, 1995, vol. 14, no. 3, p. 401.
41. Hendra, P.J. and Jovic, Z., *J. Chem. Soc.*, 1968, vol. 209, p. 600.

Translated by E. Yablonskaya